Supporting Information

An *in situ* Dual Modification Strategy for Enhancing the Electrocatalytic Oxygen Evolution Performance of ZIF-67

Rajesha Kumar Swain,[a±] *Aranya Kar,*[a±] *Aditi Halder*[a] *and Chullikkattil P. Pradeep*[a]*

[a]School of Chemical Sciences, Indian Institute of Technology Mandi, Mandi, Himachal Pradesh – 175005, India, Email: pradeep@iitmandi.ac.in; Fax: +911905 267 009; Tel: +91 1905 267 045

[±] These authors contributed equally to the manuscript

Electrochemical Methods

Fabrication of working electrodes.

The sample-modified electrodes were prepared as follows: 4 mg of the catalyst, 1 mg of acetylene black, and 10 μL of 5 wt% Nafion (aq) binder were taken in 1 mL of isopropyl alcohol (IPA)/water mixture (3:2; v/v) and sonicated until a homogeneous suspension was formed. 20 μL of this mixture was drop-casted on the 4 mm glassy carbon electrode (GCE) (geometrical area = 0.126 cm^2), resulting in a constant catalyst coating of 80 μg in all samples on the electrode surface. GCE coated with the catalyst mixture was dried under the IR lamp (temperature ~70 ° C). All the electrochemical experiments were performed at ambient temperature.

Electrochemical data analyses.

The electrocatalytic OER experiments were conducted on an electrochemical work station (CHI 760F, made in U.S.A). The working electrodes were scanned several times until the signals were stabilized, and then LSV data were collected. CV and LSV analyses were performed to confirm the electrocatalytic properties of the working electrodes.

Butler-Volmer equation was used to estimate the OER slope considering the exponential region of the obtained LSV curves. By employing the Tafel equation:

$$\eta = b \log j + a$$

Where η is the overpotential, b is the Tafel slope, j is the current density and a is the exchange current density. The Tafel slopes and exchange current densities could be calculated for composites.

In addition, the overpotential was calculated using:

$$\eta = E\ (RHE) - 1.23\ V$$

The electrochemically active surface area (ECSA) of the catalyst was calculated by the following equation:

$$ECSA = C_{dl}/C_s$$

where C_{dl} is the electrochemical double-layer capacitance calculated from cyclic voltammetry in a non-Faradaic region under variable scan rates. C_s is the specific capacitance. We used the reported value of 0.040 mF cm^{-2} for **Z67**-based system.[1]

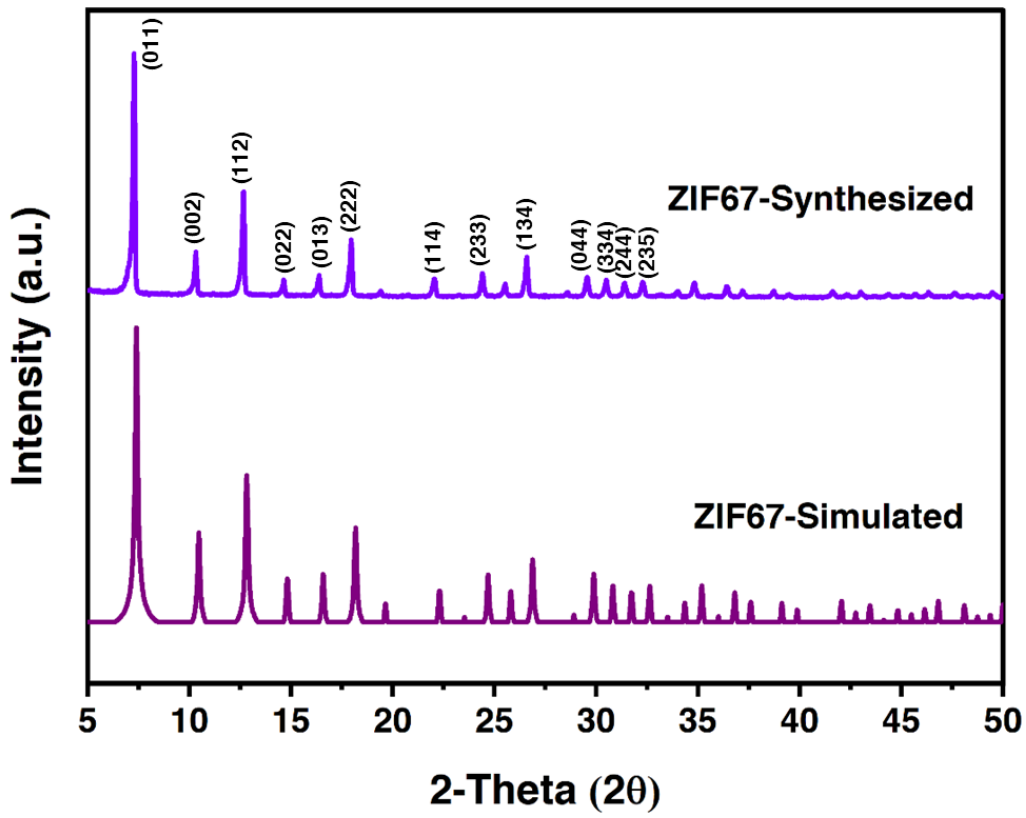

Fig. S1 XRD patterns of simulated **Z67** and synthesized **Z67.**

Table S1. BET parameters of pristine **Z67** and all three composites (**25/50/75NZ67**).

Material	Surface Area (m^2/g)	Avg. Pore diameter (nm)	Pore volume (cm^3/g)
Z67	1102.99	2.38	0.656
25NZ67	764.97	2.62	0.5
50NZ67	483.54	2.76	0.367
75NZ67	356.10	3.02	0.268

Table S2. ICP-MS data for **Z67, 25NZ67, 50NZ67** and **75NZ67**.

Sample	Co (mmol g^{-1})	V (mmol g^{-1})	Ni (mmol g^{-1})	Ni/Co	V/Co	Ni/V
Z67	4.77	—	—	—	—	—
25NZ67	5.19	0.84	0.007	0.0013	0.162	0.008
50NZ67	5.21	1.58	0.022	0.004	0.303	0.014
75NZ67	5.12	1.94	0.034	0.007	0.38	0.017

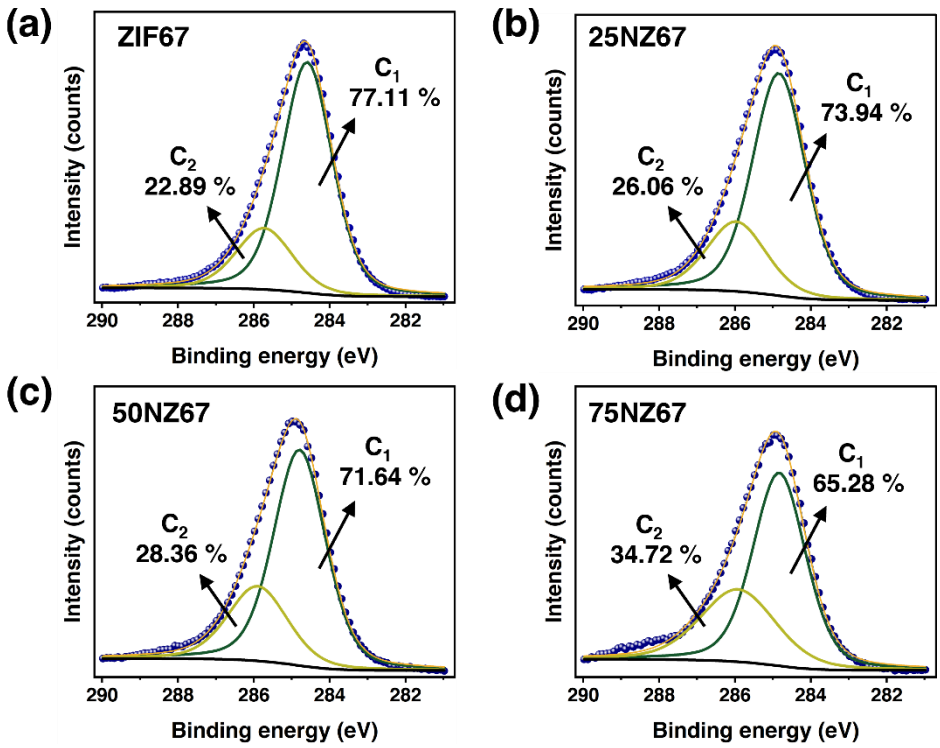

Fig. S2 C 1s XPS spectra of (a) **Z67**; (b) **25NZ67**; (c) **50NZ67** and (d) **75NZ67**.

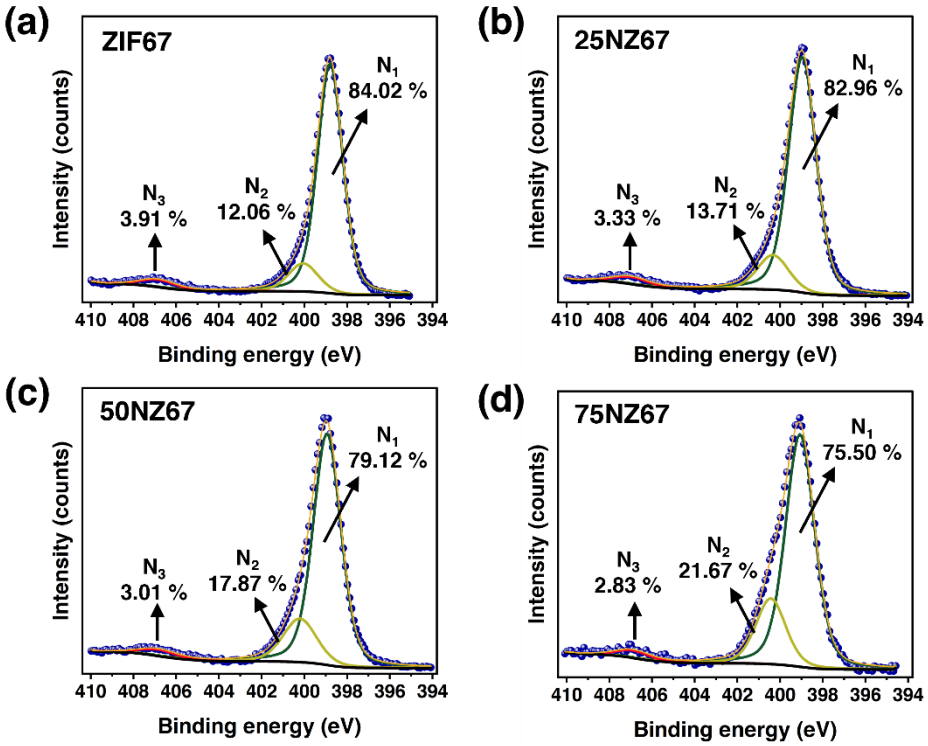

Fig. S3 N 1s XPS spectra of (a) **Z67**; (b) **25NZ67**; (c) **50NZ67** and (d) **75NZ67**.

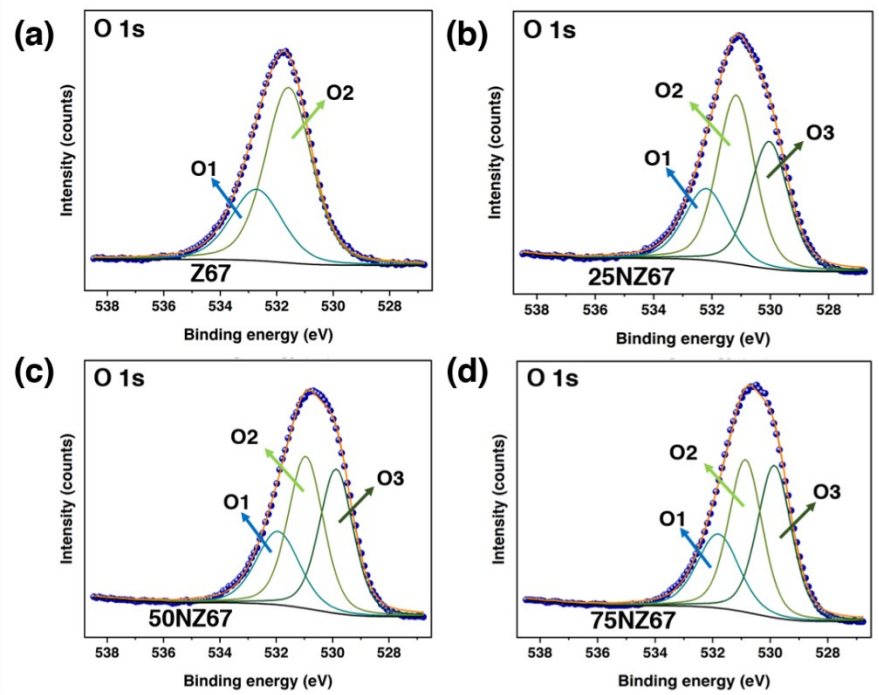

Fig. S4 O 1s XPS spectra of (a) **Z67**; (b) **25NZ67**; (c) **50NZ67** and (d) **75NZ67**.

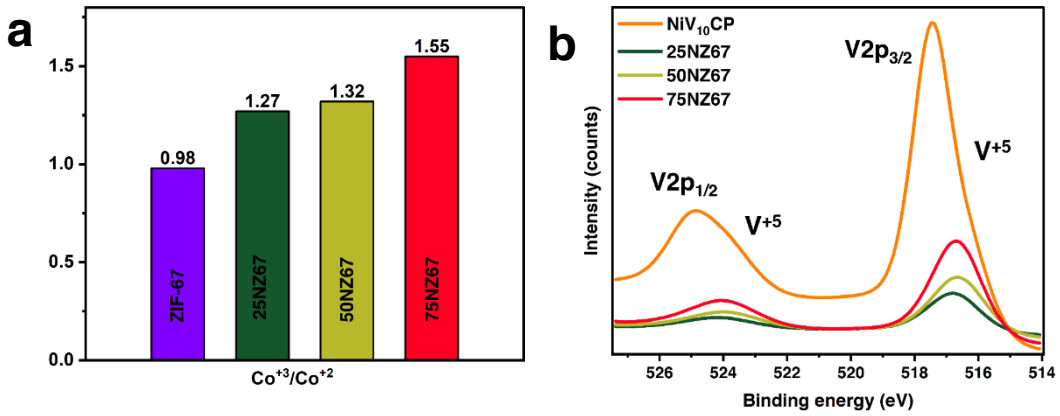

Fig. S5 (a) Co^{3+}/Co^{2+} ratio calculated from XPS analysis for **Z67** and **25/50/75NZ67** composites; and (b) Stacking of XPS high-resolution V 2p core-level peaks for **NiV_{10}** and all three composites (**25/50/75NZ67**).

Table S3. XPS atomic % data for **Z67**, **25NZ67**, **50NZ67** and **75NZ67**.

Sample	XPS atomic % (at.%)							
	C	O	N	Co	V	Ni	K	Ni/V ratio
$NiV_{10}CP$	16.84	53.50	-	-	16.59	6.08	3.17	0.36
Zif-67	61.90	14.82	15.48	7.80	-	-	-	-
25NZ67	46.44	21.87	15.38	13.82	1.82	0.43	0.24	0.23
50NZ67	41.64	26.28	13.59	14.79	2.92	0.52	0.26	0.17
75NZ67	31.94	37.72	7.39	17.50	4.63	0.59	0.23	0.12

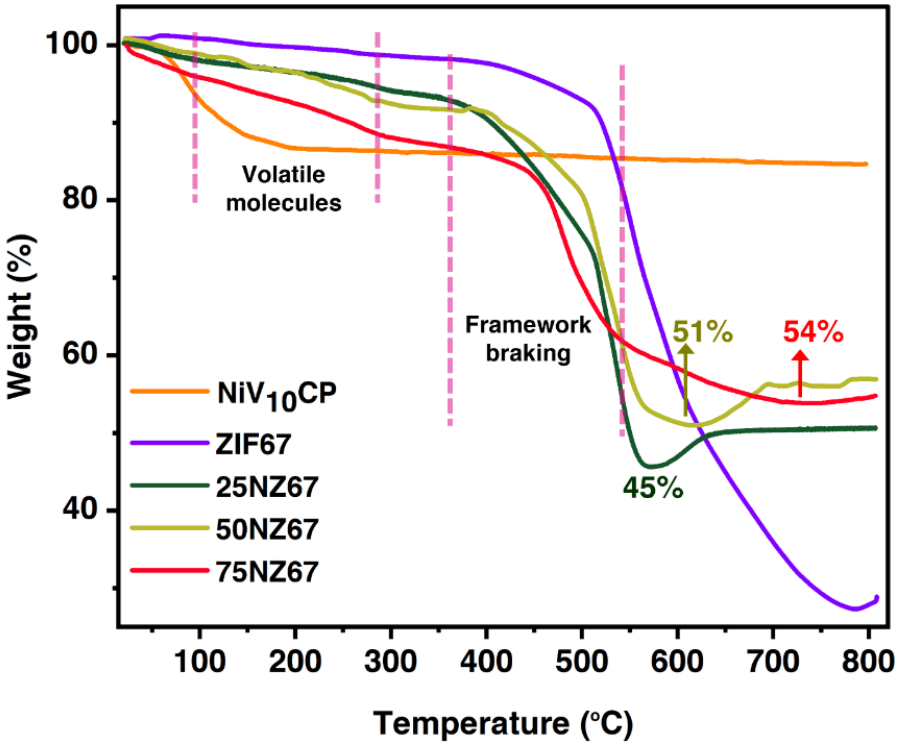

Fig. S6 Thermogravimetric analysis of **Z67**, **NiV$_{10}$**, **25NZ67**, **50NZ67** and **75NZ67**.

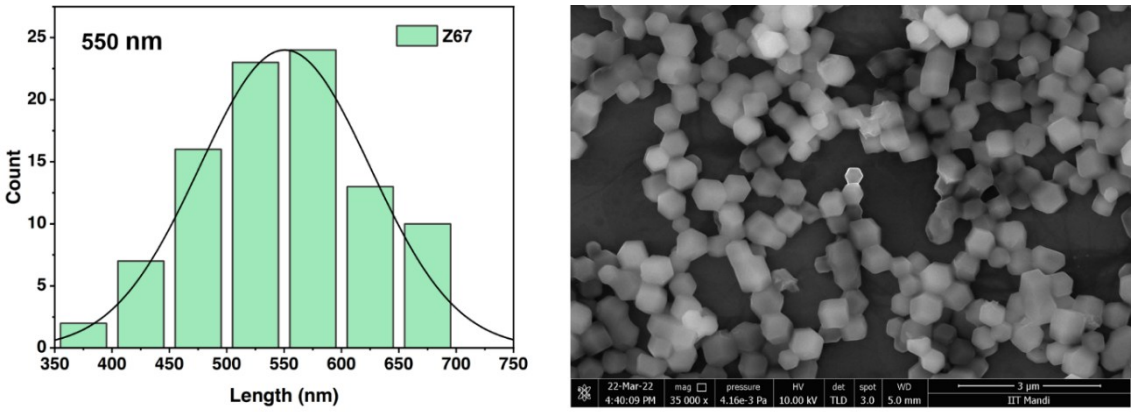

Fig. S7 Size distribution of **Z67** particles calculated using ImageJ software and the corresponding FESEM image used for calculation.

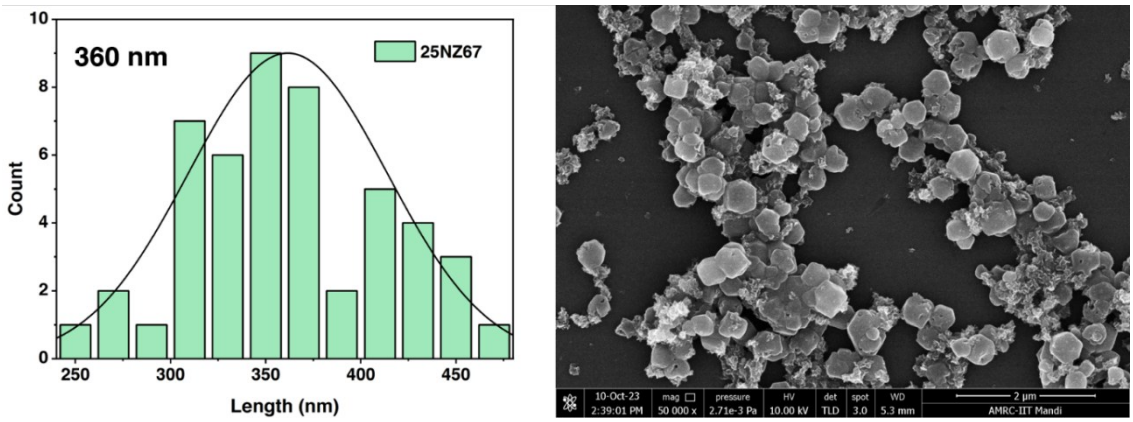

Fig. S8 Size distribution of **25NZ67** particles calculated using ImageJ software and the corresponding FESEM image used for calculation.

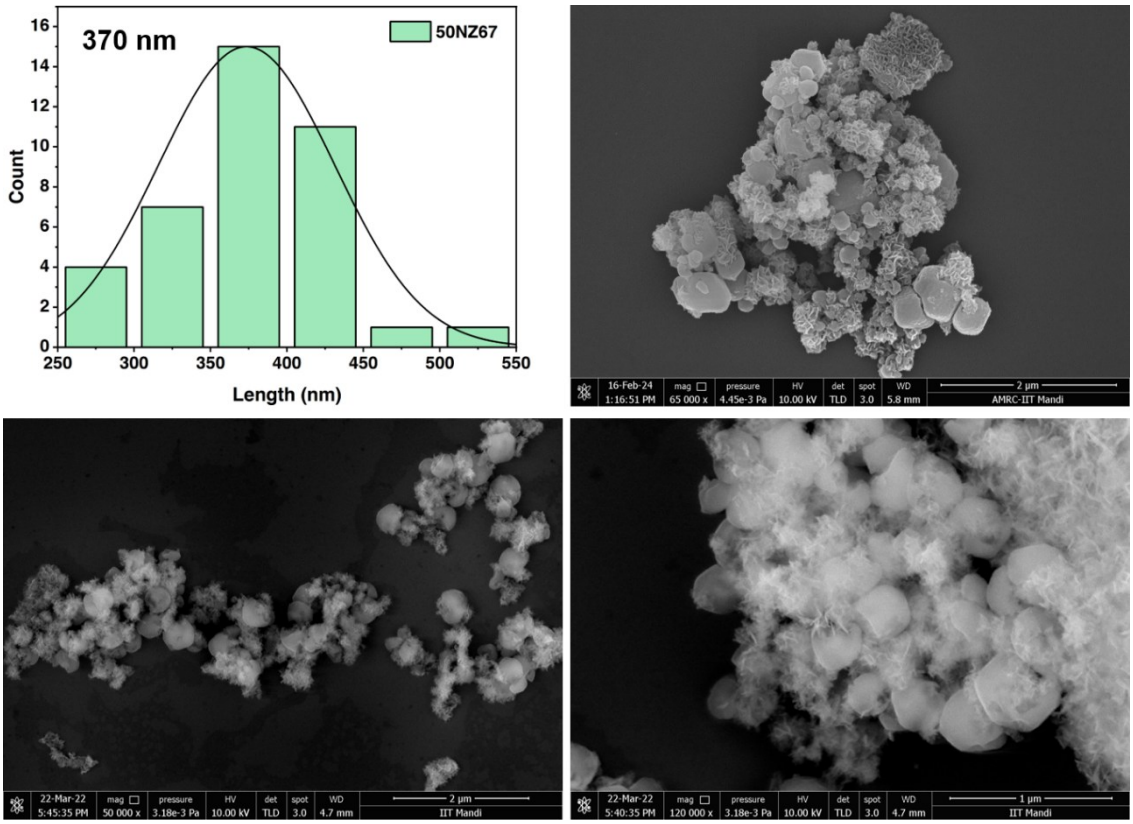

Fig. S9 Size distribution of **50NZ67** particles calculated using ImageJ software and the corresponding FESEM images used for calculation.

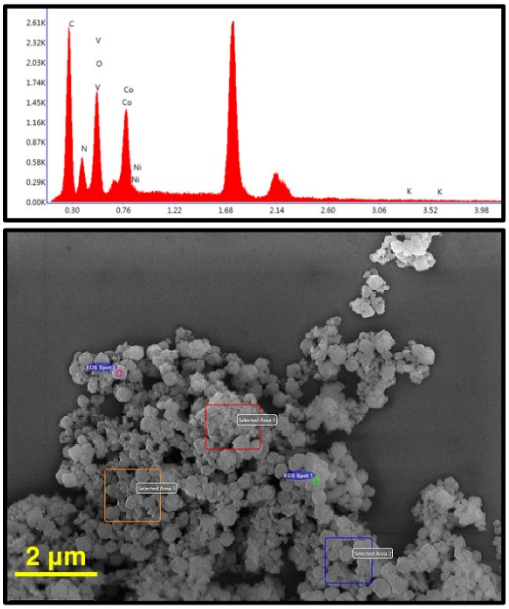

Elements	Weight %	Atomic %
C K	29.32	47.13
N K	12.67	17.39
V L	18.83	7.15
O K	17.61	21.17
CoL	20.70	6.79
NiL	0.45	0.16
K K	0.43	0.21
Total	100	100

Fig. S10 EDX spectra of **25NZ67** composite.

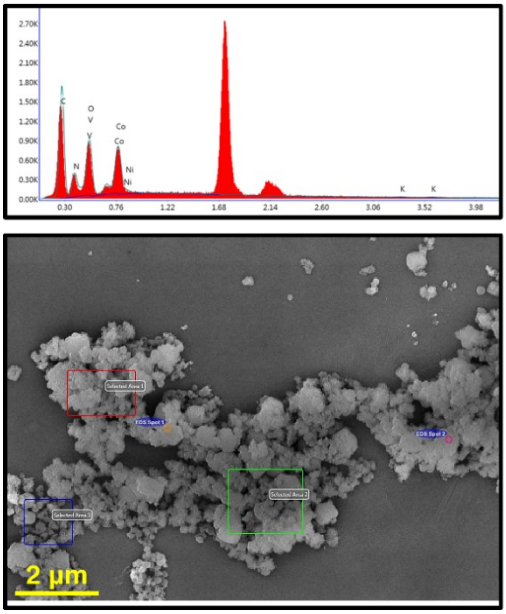

Elements	Weight %	Atomic %
C K	25.78	44.65
N K	9.42	14.10
V L	23.32	9.54
O K	18.02	23.33
CoL	22.03	7.76
NiL	0.76	0.25
K K	0.68	0.36
Total	100	100

Fig. S11 EDX spectra of **50NZ67** composite.

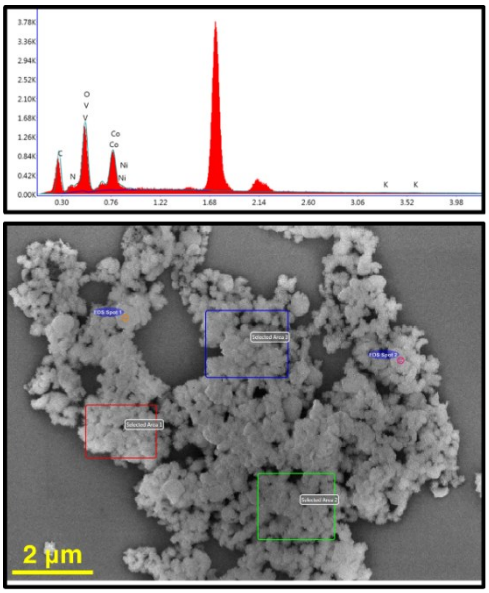

Elements	Weight %	Atomic %
C K	17.12	33.72
N K	4.08	6.89
V L	26.94	12.51
O K	24.10	35.64
CoL	25.54	10.25
NiL	1.71	0.69
K K	0.51	0.31
Total	100	100

Fig. S12 EDX spectra of **75NZ67** composite.

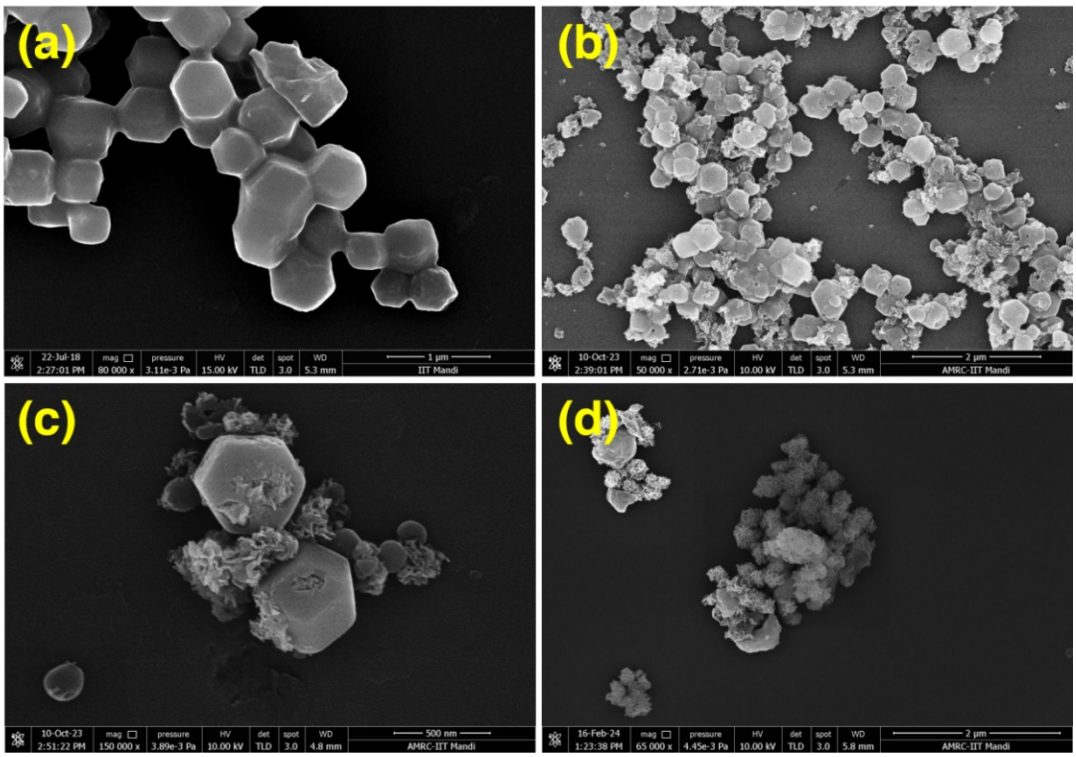

Fig. S13 FESEM images of (a) **Z67**; (b) **25NZ67**; (c) **50NZ67** and (d) **75NZ67**.

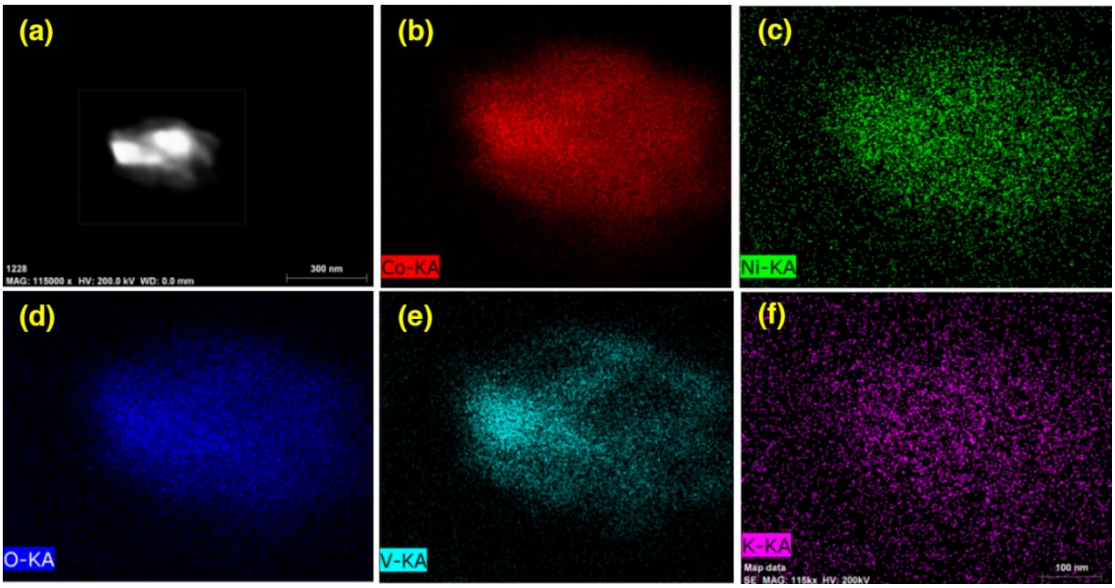

Fig. S14 Elemental mapping of **25NZ67** showing (a) mapping area; (b) Co map; (c) Ni map; (d) O map; (e) V map; and (f) K map.

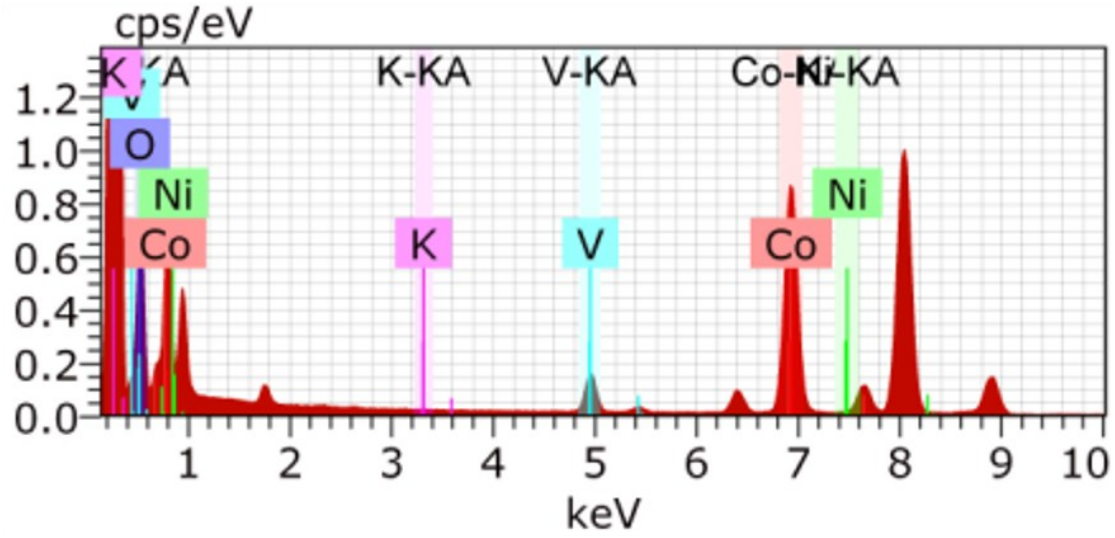

Fig. S15 EDX of the mapping area of S14 (a).

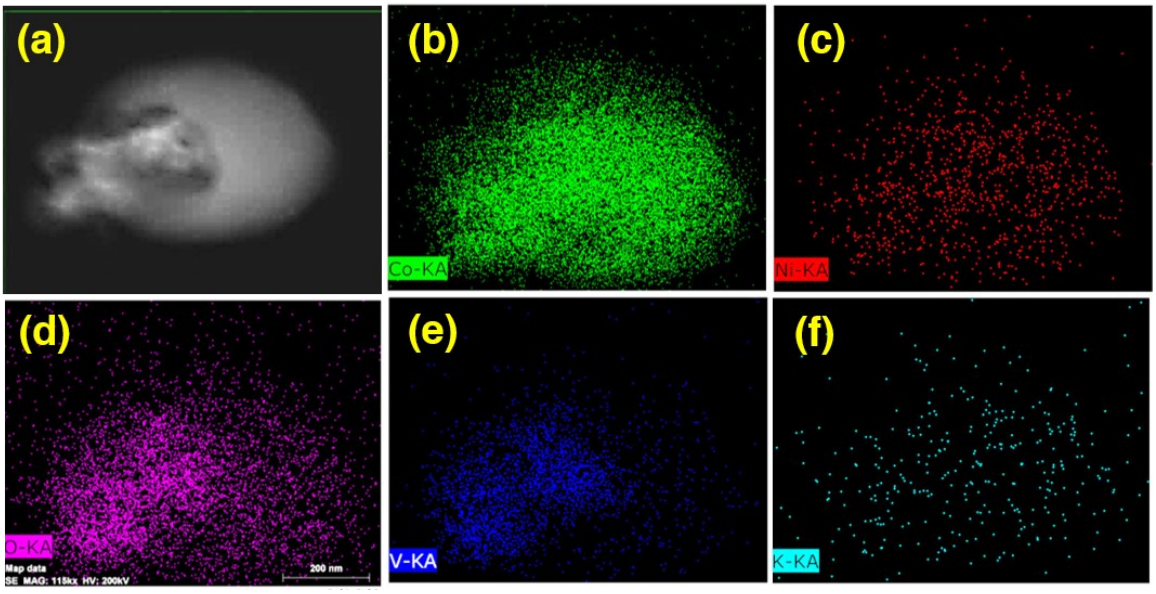

Fig. S16 Elemental mapping of **50NZ67** showing (a) mapping area; (b) Co map; (c) Ni map; (d) O map; (e) V map and (f) K map.

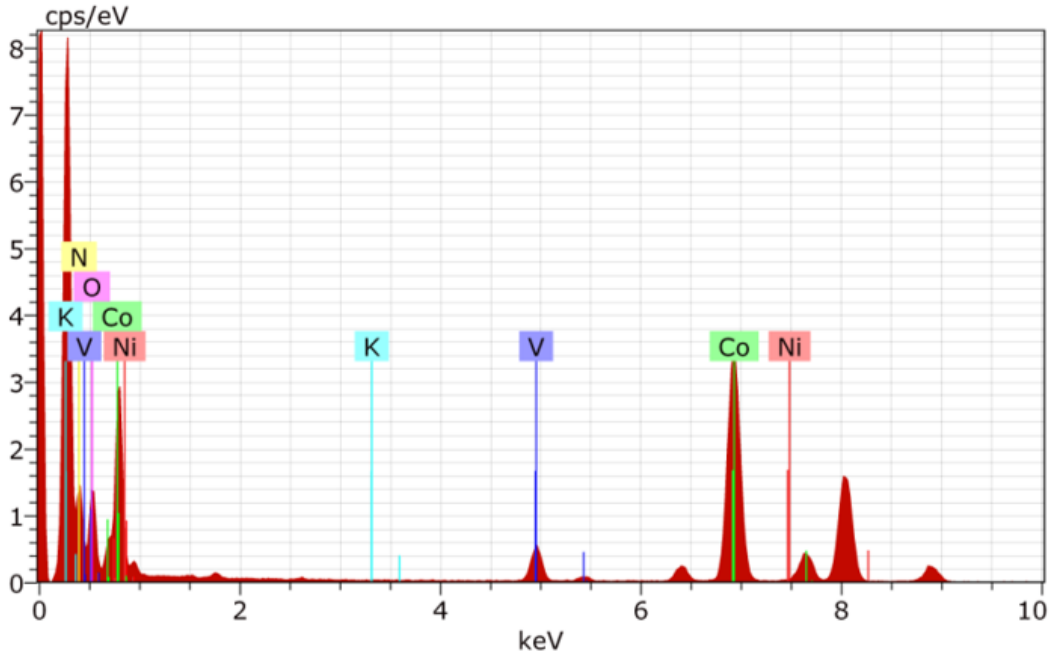

Fig. S17 EDX of the mapping area of S16 (a).

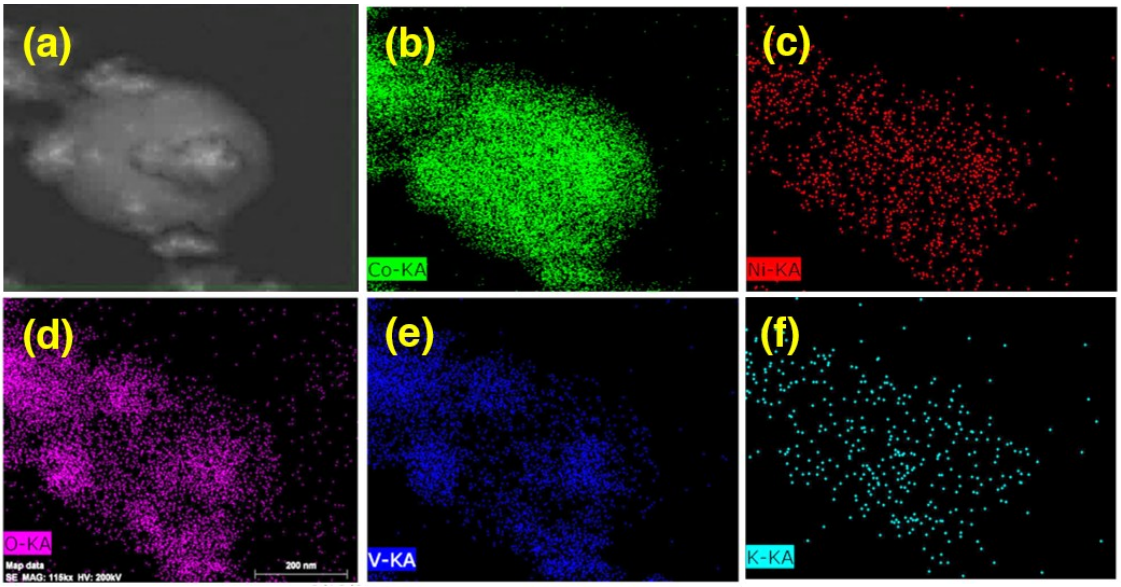

Fig. S18 Elemental mapping of **75NZ67** showing (a) mapping area; (b) Co map; (c) Ni map; (d) O map; (e) V map and (f) K map.

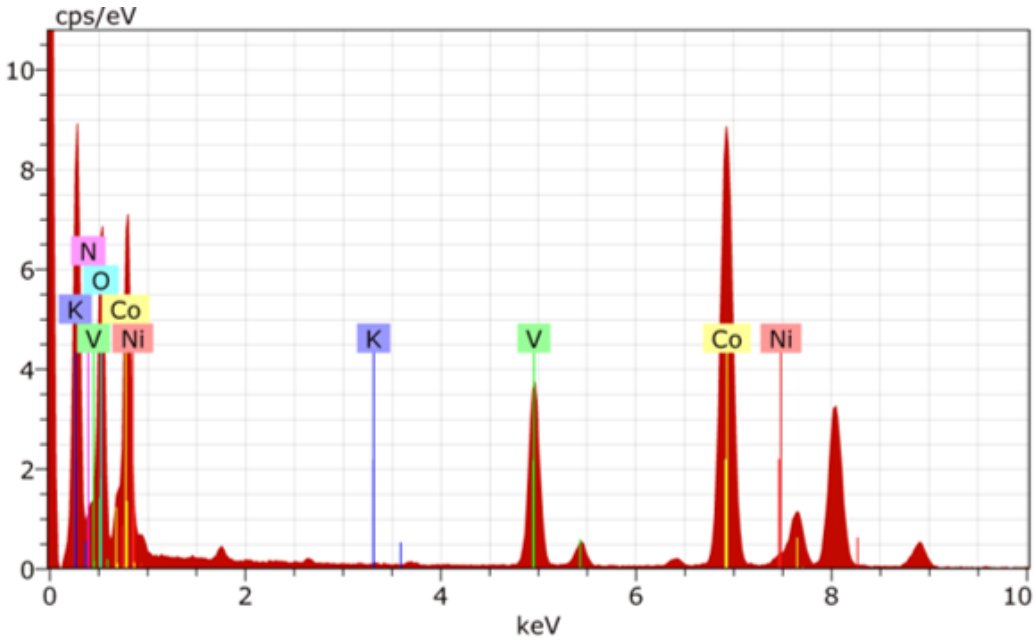

Fig. S19 EDX of the mapping area of S18 (a).

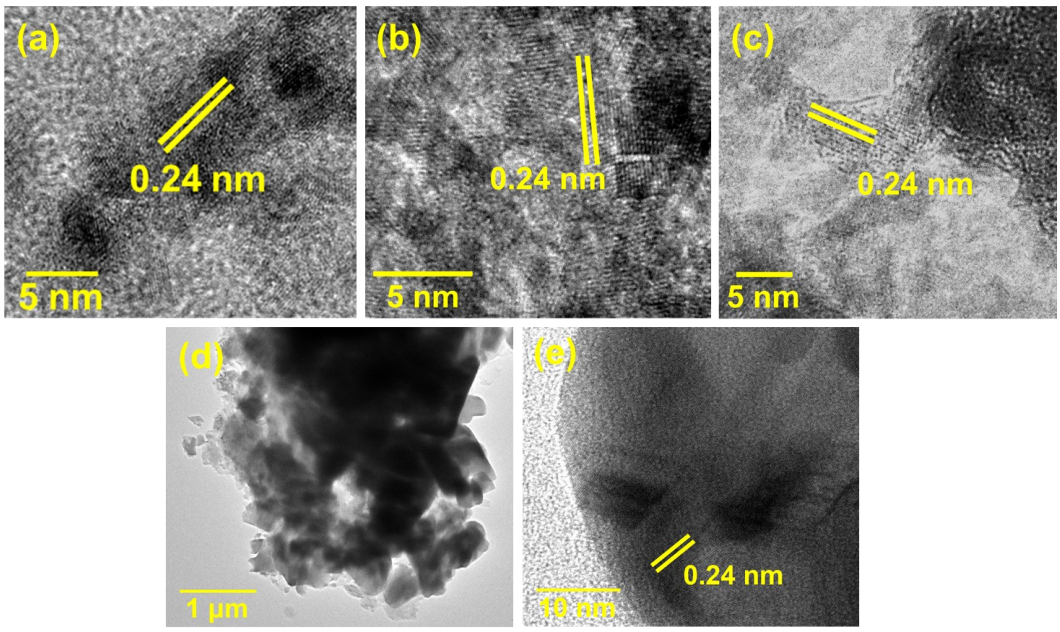

Fig. S20 HRTEM of (a) **25NZ67**; (b) **50NZ67** and (c) **75NZ67** showing d-spacing of 0.24 nm; (d) TEM image of sodium salt of V_{10} POM, and (e) HRTEM of sodium salt of V_{10} POM showing d-spacing of 0.24 nm.

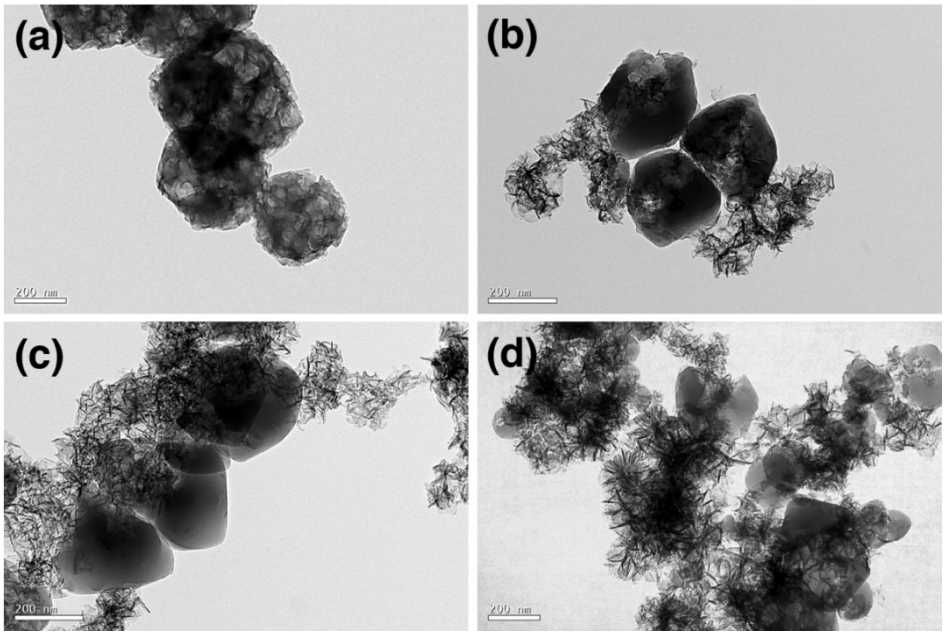

Fig. S21 TEM images of (a) **Z67**; (b) **25NZ67**; (c) **50NZ67** and (d) **75NZ67**.

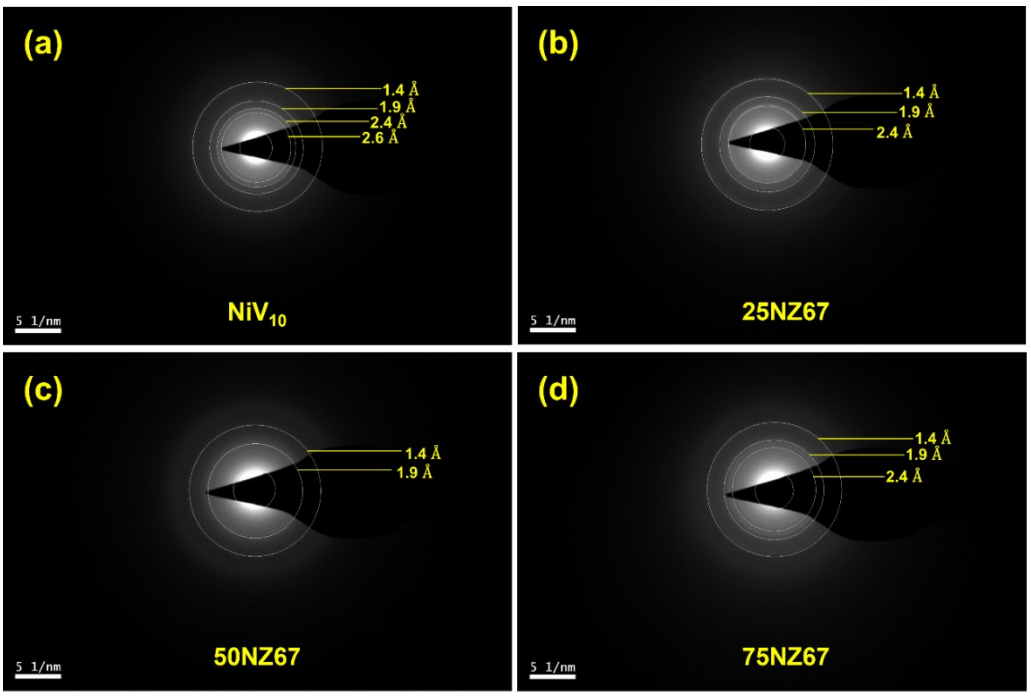

Fig. S22 SAED patterns of (a) **NiV_{10}** (d-spacing of 2.6, 2.4, 1.9 and 1.4 Å); (b) **25NZ67** (d-spacing of 2.4, 1.9 and 1.4 Å); (c) **50NZ67** (d-spacing of 1.9 and 1.4 Å) and (d) **75NZ67** (d-spacing of 2.4, 1.9 and 1.4 Å).

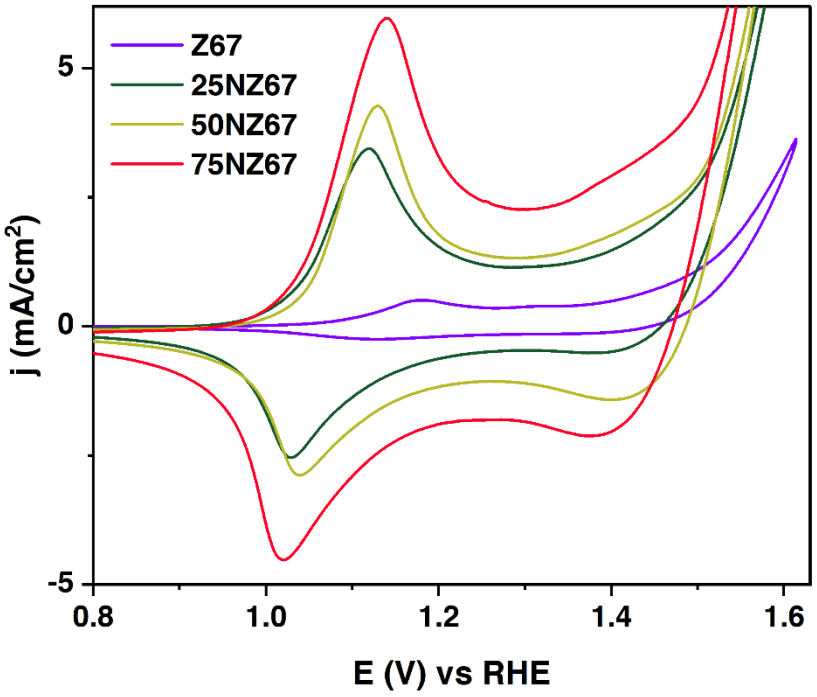

Fig. S23 Cyclic voltammograms (CVs) of all three composites (**25/50/75NZ67**), and **Z67** in 0.1M KOH.

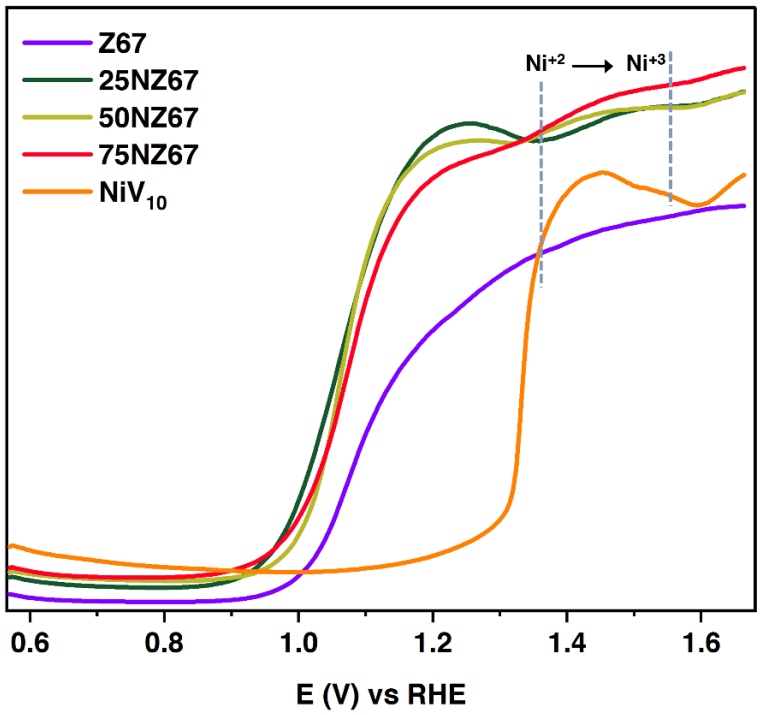

Fig. S24 Differential pulse voltammograms (DPVs) of three composites (**25/50/75NZ67**), **Z67** and **NiV_{10}** in 0.1M KOH.

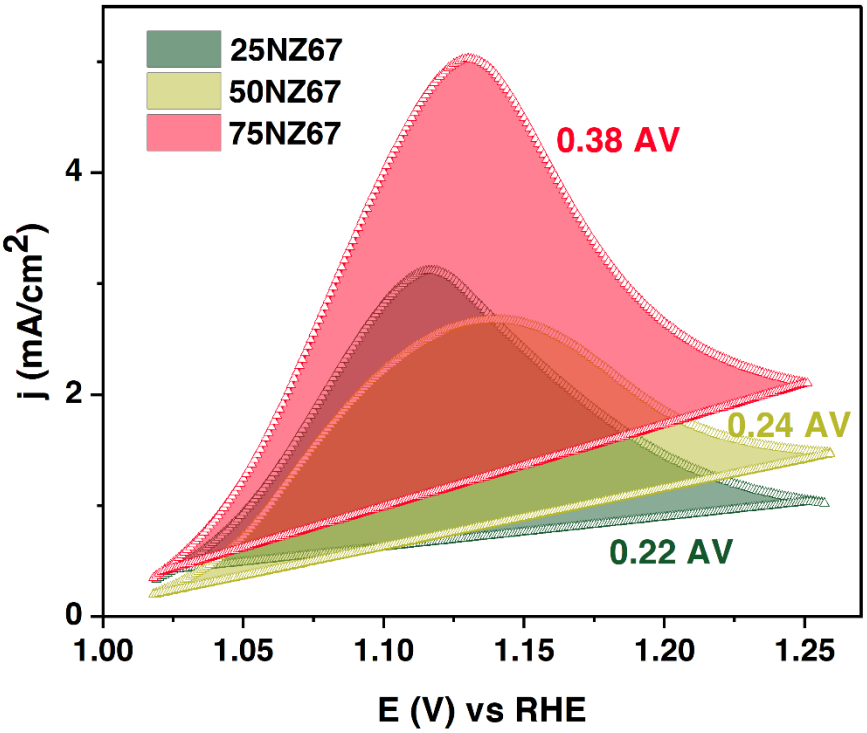

Fig. S25 Area under the curves for relative quantification of the active species in the three composites, **25/50/75NZ67**.

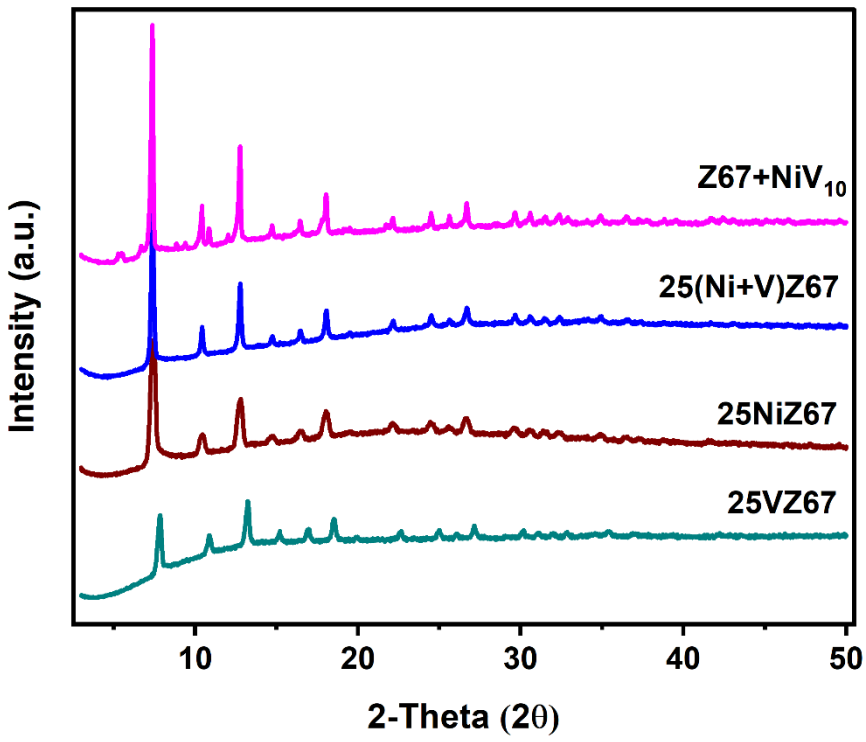

Fig. S26 XRD patterns of **25VZ67**, **25NiZ67**, **25(Ni+V)Z67** and **Z67+NiV$_{10}$**.

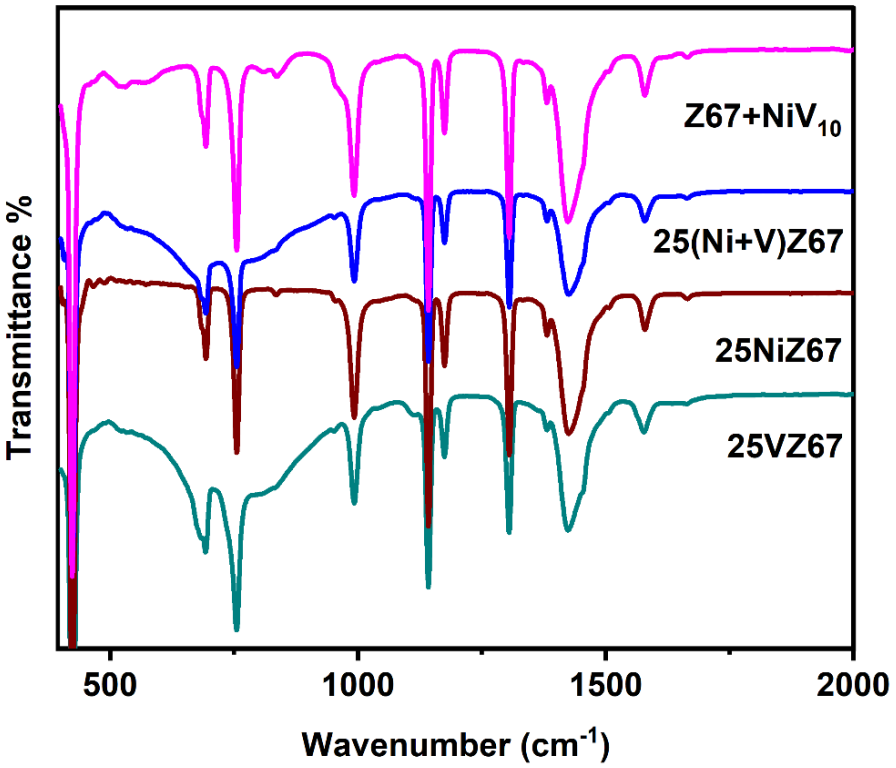

Fig. S27 FT-IR spectra of **25VZ67**, **25NiZ67**, **25(Ni+V)Z67** and **Z67+NiV$_{10}$**.

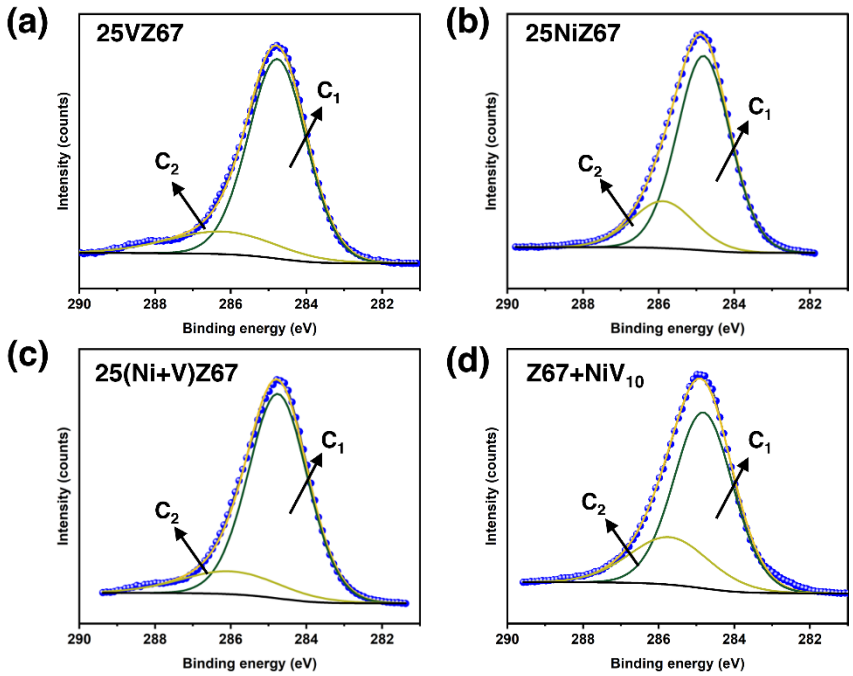

Fig. S28 C 1s XPS spectra of (a) **25VZ67**; (b) **25NiZ67**; (c) **25(Ni+V)Z67** and (d) **Z67+NiV$_{10}$**.

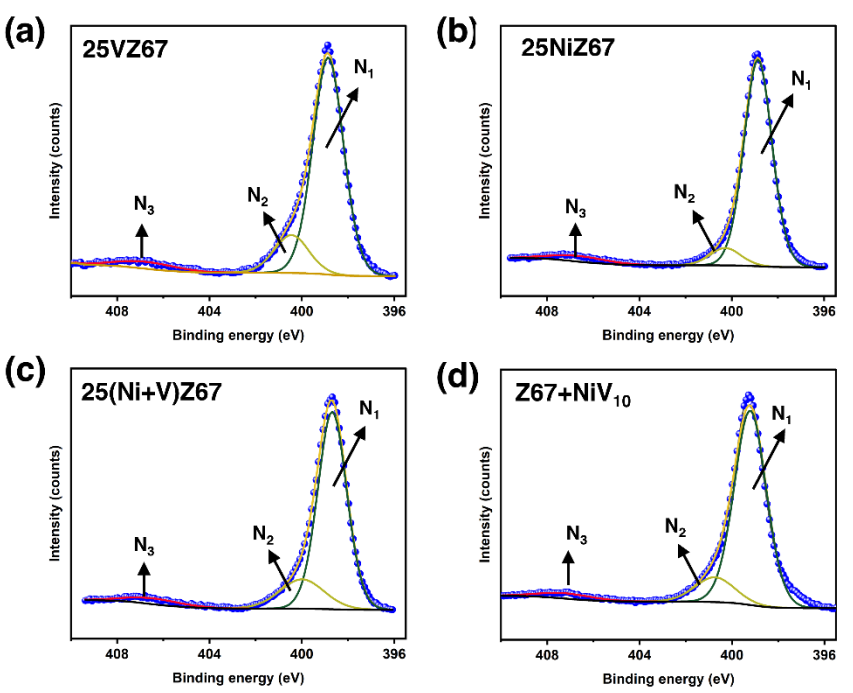

Fig. S29 N 1s XPS spectra of (a) **25VZ67**; (b) **25NiZ67**; (c) **25(Ni+V)Z67** and (d) **Z67+NiV$_{10}$**.

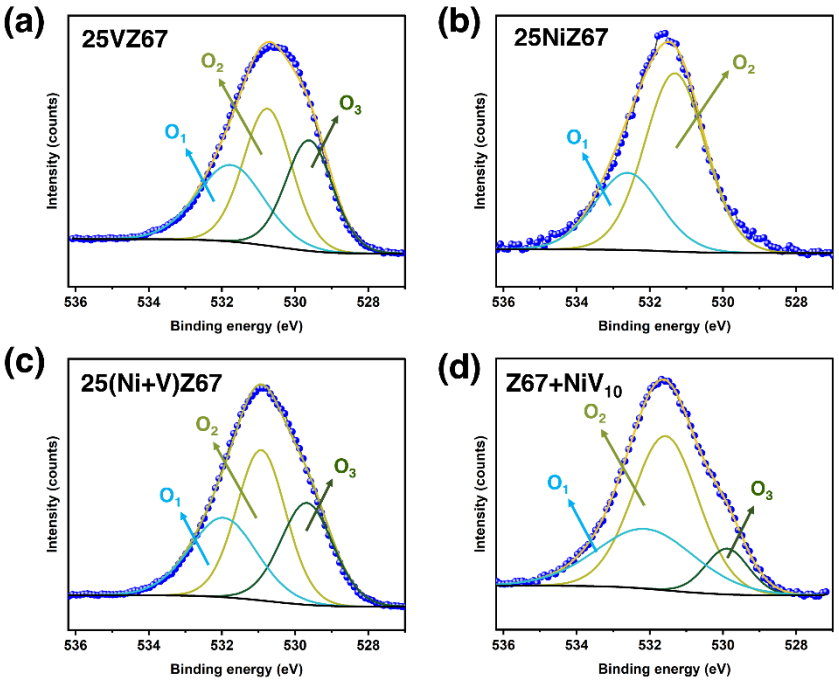

Fig. S30 O 1s XPS spectra of (a) **25VZ67**; (b) **25NiZ67**; (c) **25(Ni+V)Z67** and (d) **Z67+NiV$_{10}$**.

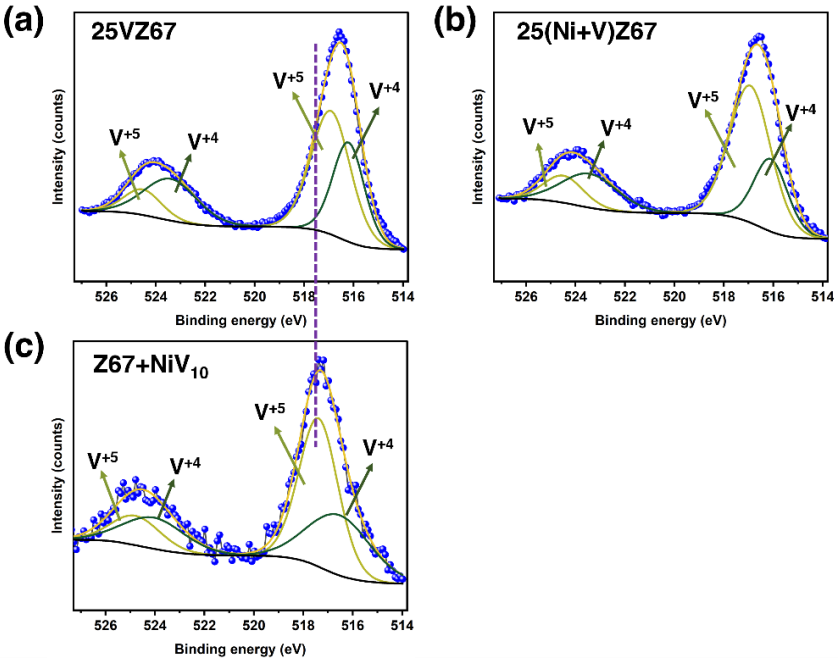

Fig. S31 V 2p XPS spectra of (a) **25VZ67**; (b) **25(Ni+V)Z67**; and (c) **Z67+NiV$_{10}$**.

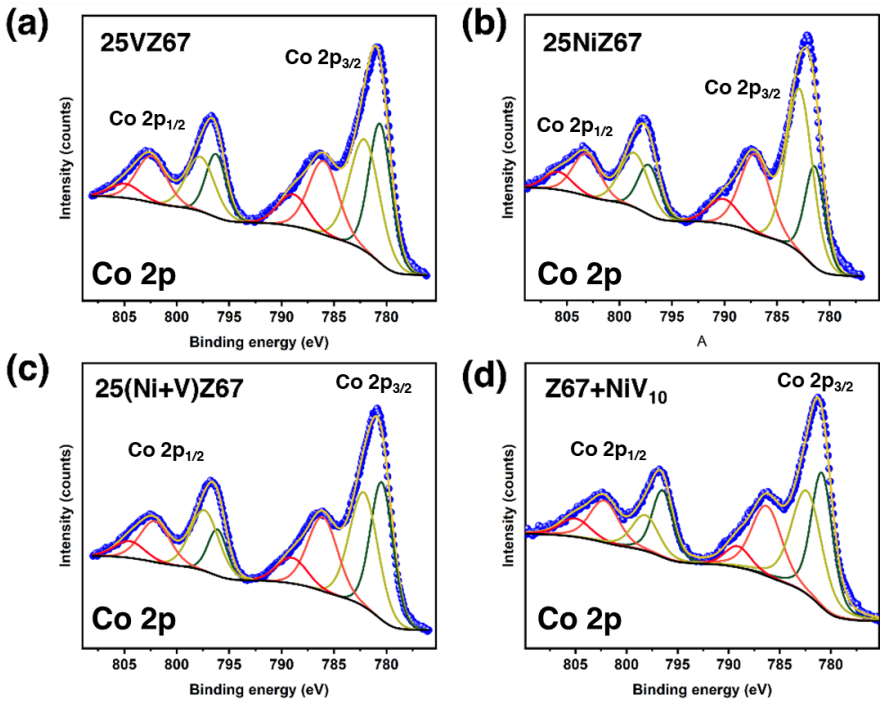

Fig. S32 Co 2p XPS spectra of (a) **25VZ67**; (b) **25NiZ67**; (c) **25(Ni+V)Z67** and (d) **Z67+NiV$_{10}$**.

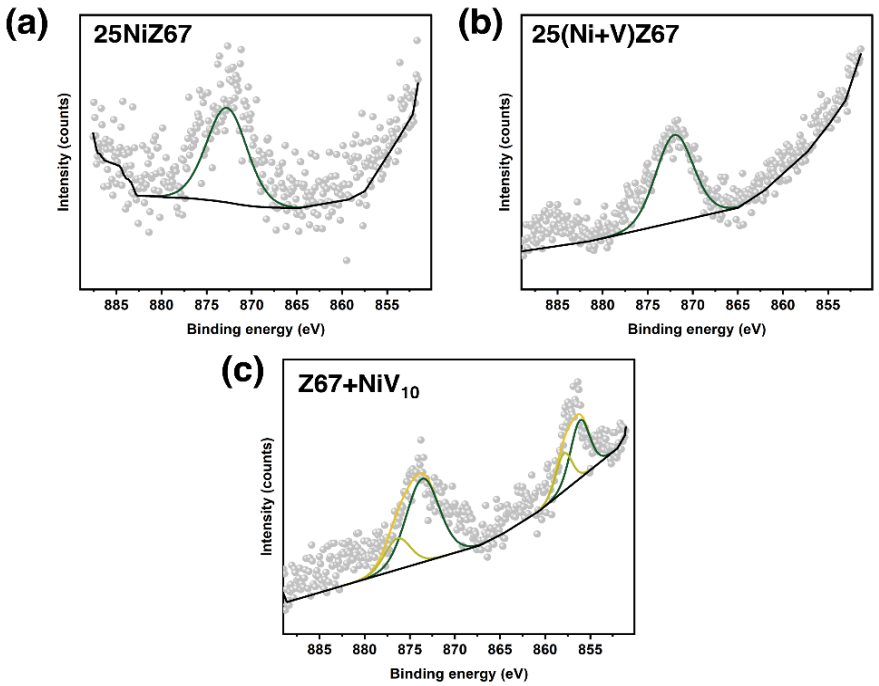

Fig. S33 Ni 2p XPS spectra of (a) **25NiZ67**; (b) **25(Ni+V)Z67** and (c) **Z67+NiV$_{10}$**.

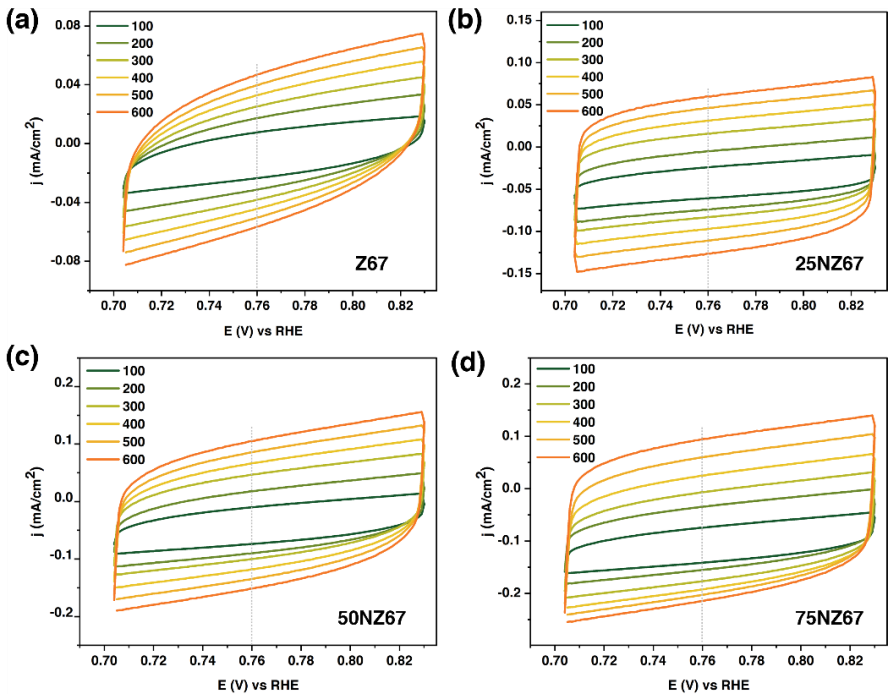

Fig. S34 C_{dl} calculation in the non-faradic region of (a) **25NZ67**; (b) **50NZ67**; (c) **75NZ67** and (d) **Z67** at variable scan rates of 100-600 mV/s.

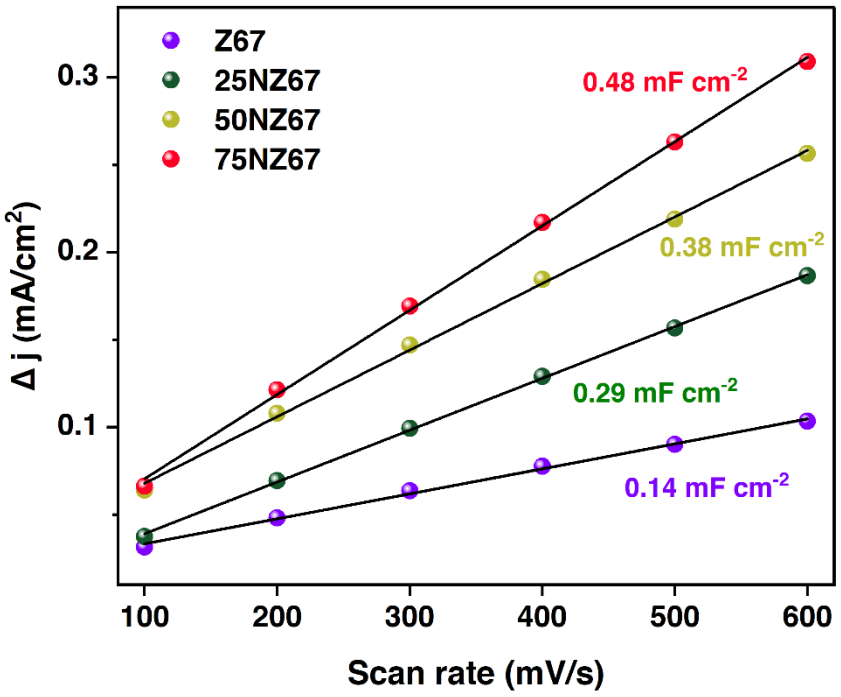

Fig. S35 C_{dl} calculation of **Z67** and **25/50/75NZ67**.

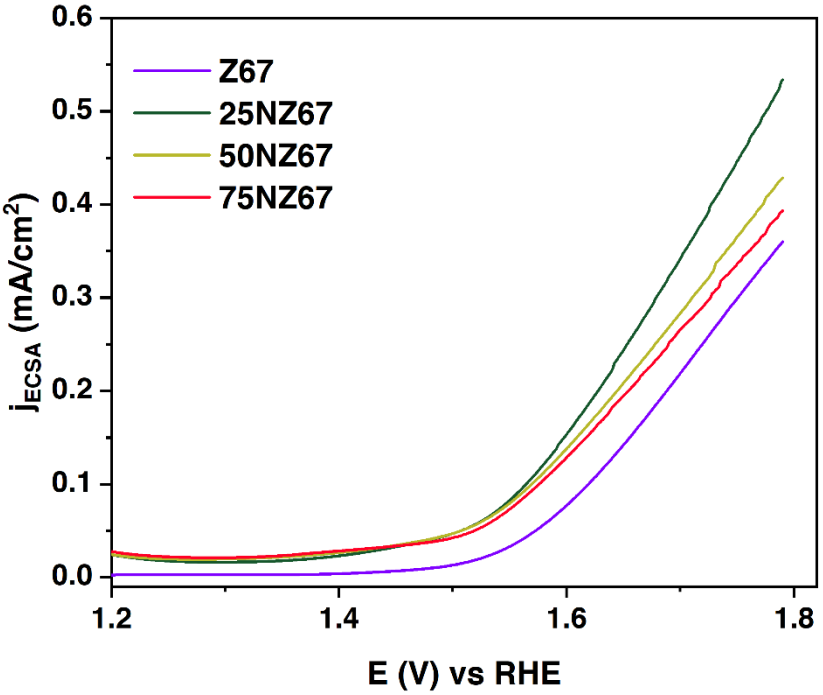

Fig. S36 ECSA normalized current density vs. potential curves for **Z67** and **25/50/75NZ67**, showing the intrinsic activity of the materials.

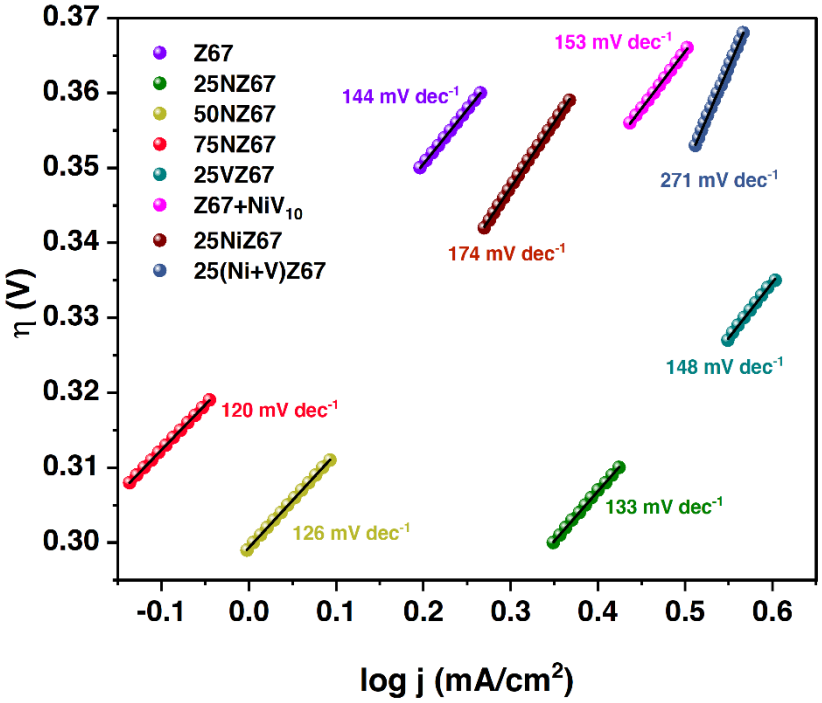

Fig. S37 Tafel slopes of **Z67**, **25/50/75NZ67** and the control samples (**25VZ67**, **Z67+NiV$_{10}$**, **25NiZ67**, and **25(Ni+V)Z67**.

Table S4. EIS circuit fitting parameters for **Z67**, **25NZ67**, **50NZ67** and **75NZ67**.

Composites	R_s	R_{ct}	C_{dl}
ZIF67	86.43 Ω	172.60 Ω	0.98 mF
25NZ67	80.75 Ω	50.05 Ω	3.86 mF
50NZ67	78.65 Ω	47.61 Ω	4.66 mF
75NZ67	77.27 Ω	44.06 Ω	5.27 mF

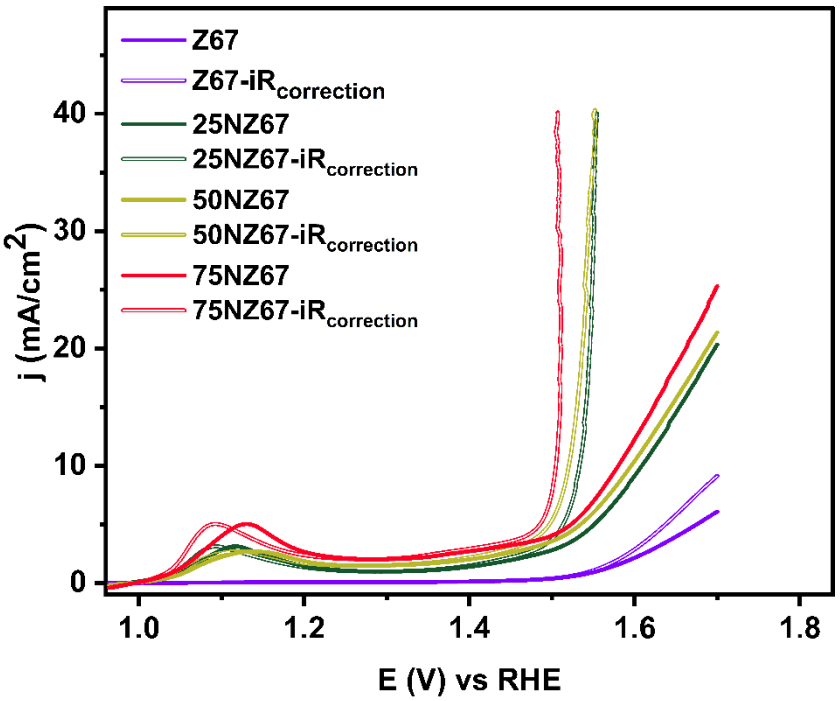

Fig. S38 LSV scans of **Z67** and **25-75NZ67** composites, along with their iR-corrected LSV curves.

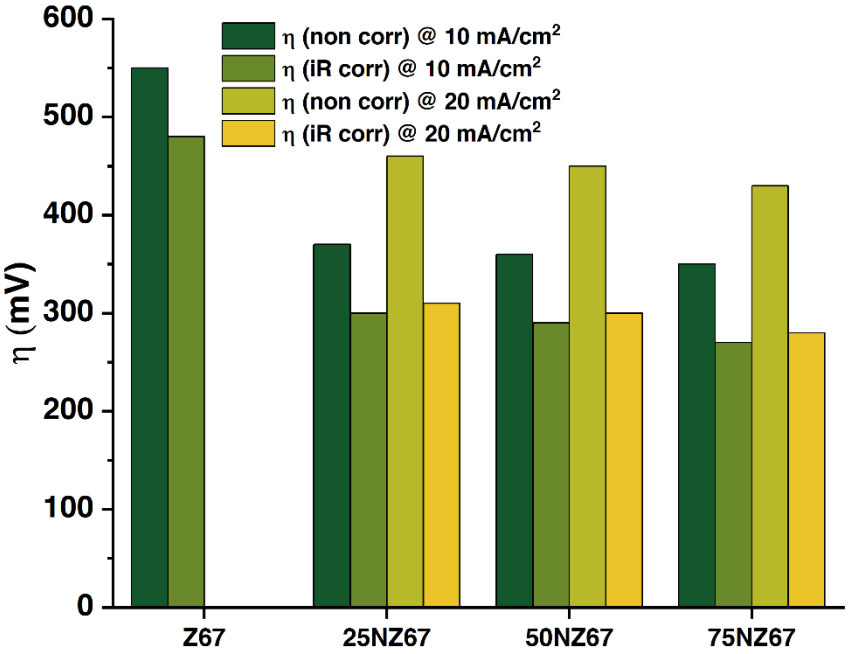

Fig. S39 Comparison of the iR-corrected and non-corrected overpotential values of the electrocatalysts at j = 10 mA/cm^2 and 20 mA/cm^2.

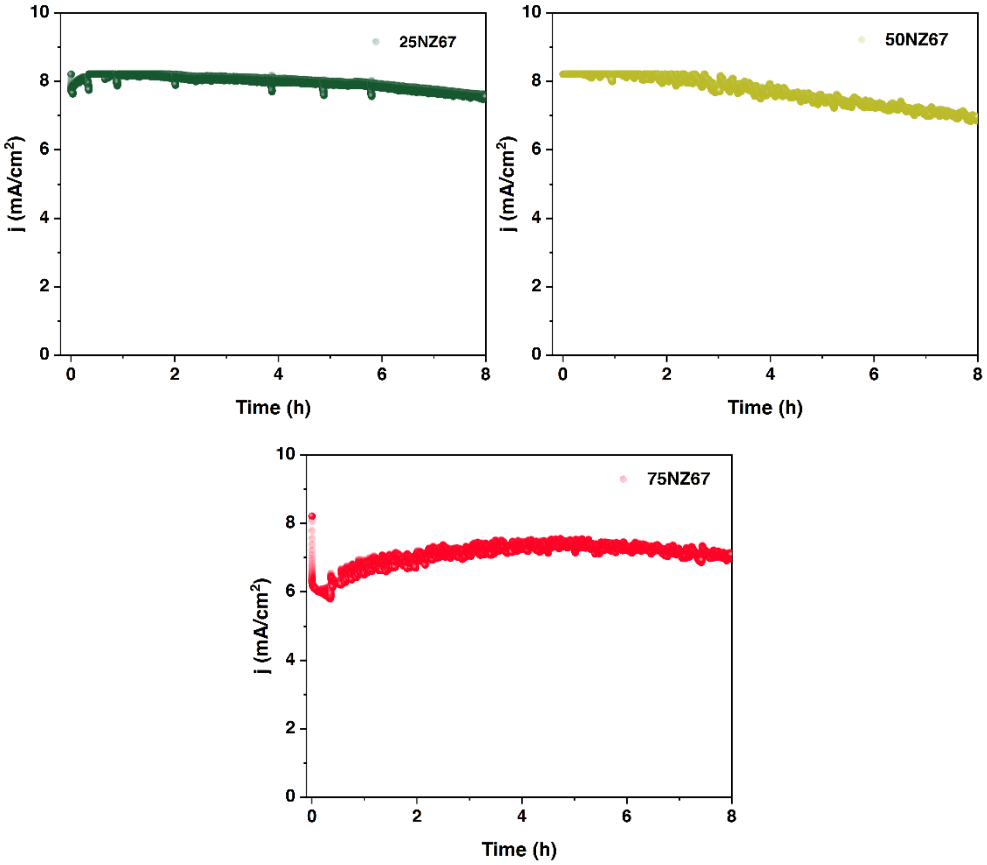

Fig. S40 8 h chronoamperometry of **25/50/75NZ67**.

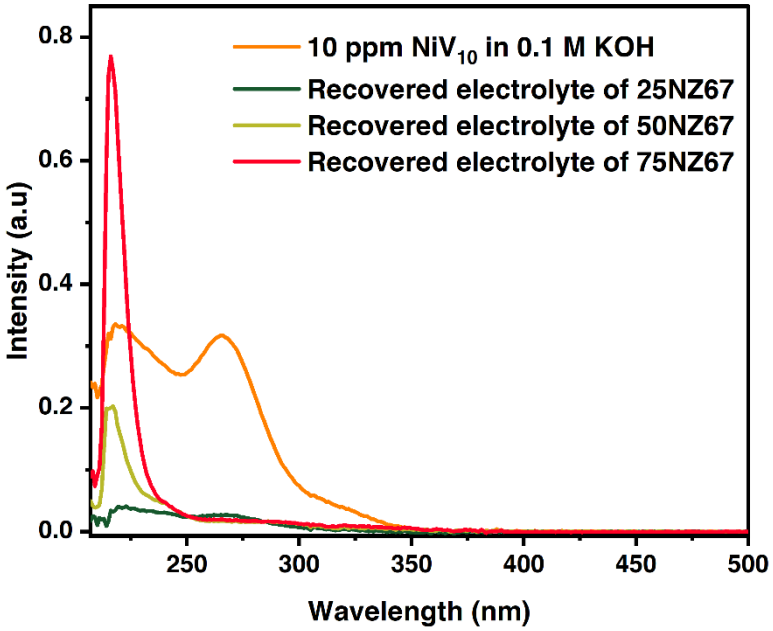

Fig. S41 UV-Vis spectra of the recovered electrolyte after 8 hours of chronoamperometry for the composites, and a 10-ppm concentration of **NiV_{10}** in 0.1 M KOH. The 0.1 M KOH was used to create the baseline during the UV-Vis spectra experiment.

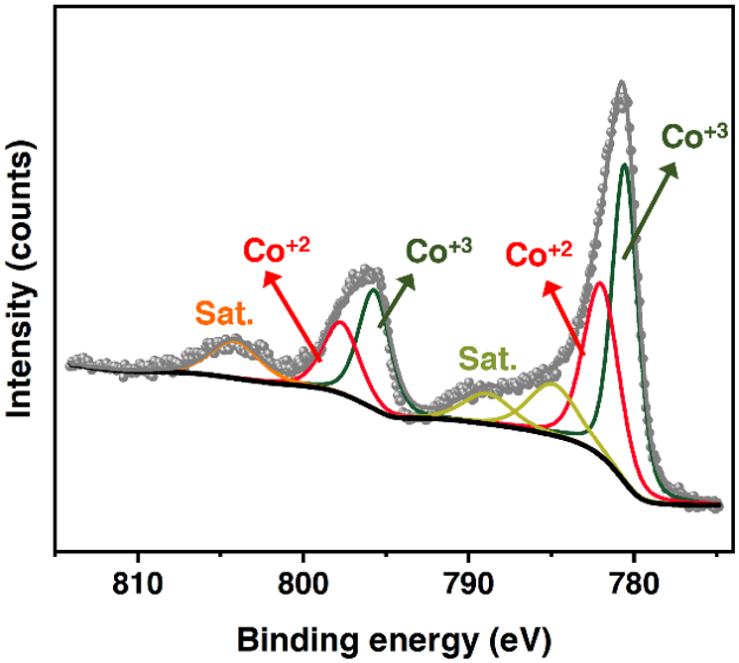

Fig. S42 Deconvoluted Co 2p scan of recovered **25NZ67** after 8 h chronoamperometry.

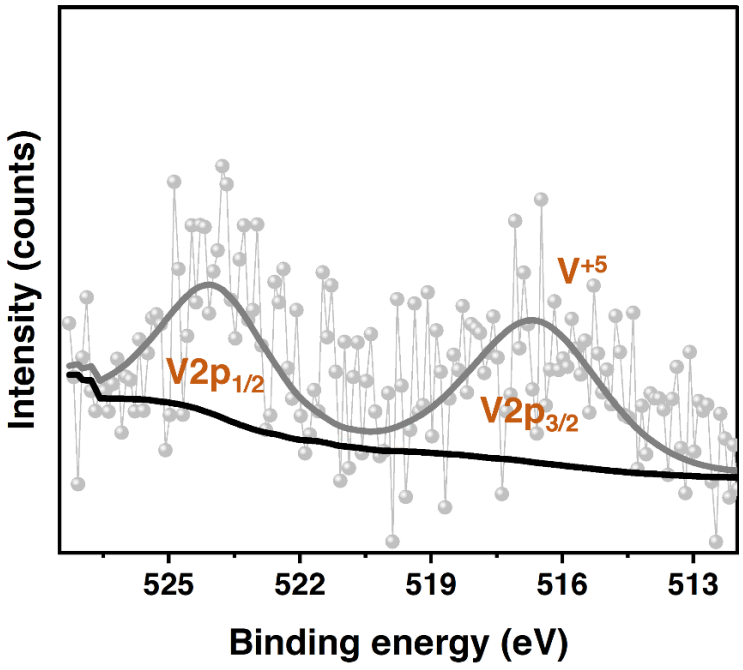

Fig. S43 Deconvoluted V 2p scan of **25NZ67** composite after 8 hr chronoamperometry.

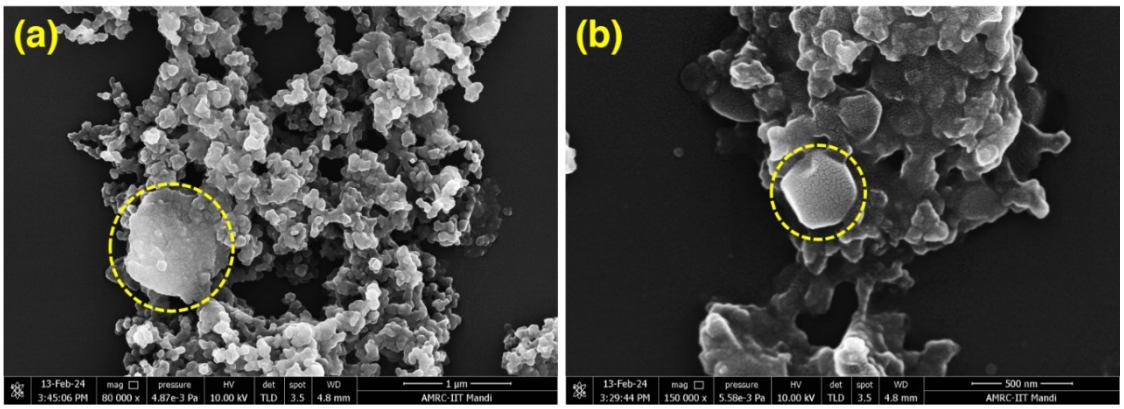

Fig. S44 FESEM images of recovered **25NZ67**, yellow dashed regions showing **Z67** polyhedra.

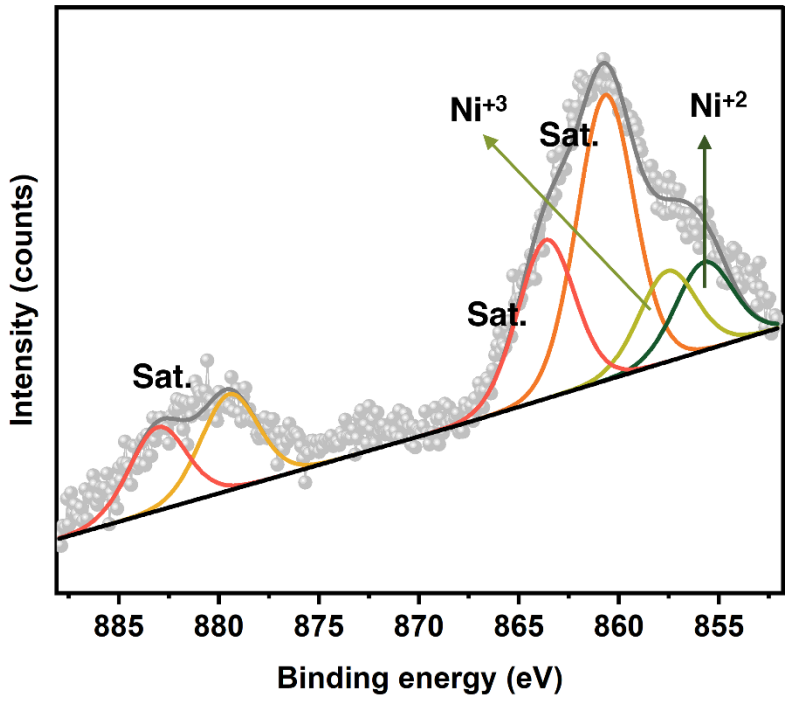

Fig. S45 Deconvoluted Ni 2p scan of **25NZ67** composite after 8 hr chronoamperometry.

Table S5. Comparison of similar ZIF based catalysts for electrocatalytic OER.

Sr. No.	Material	Electrolyte	η @ 10 (mA/cm^2)	Tafel slope (mV dec^{-1})	Ref.
1.	**ZIF-67@POM**	1.0 M KOH	287	58	2
2.	**Ti@TiO$_2$/CdS/ZIF-67**	0.5 M KOH	287	42	3
3.	**CoNiP/NC700**	1.0 M KOH	300	66	4
4.	**Co-ZIF-9**	0.1 M KOH	510	93	5
5.	**ZIF-67/NPC-2 (2:1)**	0.1 M KOH	410	114	6
6.	**ZIF-8@ZIF-67@POM**	1.0 M KOH	490	88	7
7.	**SiW9Co3[h]@ZIF-67**	0.1 M KOH	420	94	8
8.	**SiW9Co3@ZIF-67**	0.1 M KOH	470	114	9
9.	**25NZ67**	0.1 M KOH	370	133	***This work***
10.	**50NZ67**	0.1 M KOH	360	126	***This work***
11.	**75NZ67**	0.1 M KOH	350	120	***This work***

References

1. X. Li, S. You, J. Du, Y. Dai, H. Chen, Z. Cai, N. Ren and J. Zou, *Journal of Materials Chemistry A*, 2019, **7**, 25853-25864.

2. Q. Y. Li, L. Zhang, Y. X. Xu, Q. Li, H. Xue and H. Pang, *ACS Sustainable Chemistry & Engineering*, 2019, **7**, 5027-5033.

3. T. Zhang, J. Du, H. Zhang and C. Xu, *Electrochimica Acta*, 2016, **219**, 623-629.

4. J. Li, G. Du, X. Cheng, P. Feng and X. Luo, *Chinese Journal of Catalysis*, 2018, **39**, 982-987.

5. S. Wang, Y. Hou, S. Lin and X. Wang, *Nanoscale*, 2014, **6**, 9930-9934.

6. H. Wang, F.-X. Yin, B.-H. Chen, X.-B. He, P.-L. Lv, C.-Y. Ye and D.-J. Liu, *Applied Catalysis B: Environmental*, 2017, **205**, 55-67.

7. Y. Wang, Y. Wang, L. Zhang, C.-S. Liu and H. Pang, *Inorganic Chemistry Frontiers*, 2019, **6**, 2514-2520.

8. V. K. Abdelkader-Fernández, D. M. Fernandes, S. S. Balula, L. Cunha-Silva and C. Freire, *Journal of Materials Chemistry A*, 2020, **8**, 13509-13521.

9. V. K. Abdelkader-Fernández, D. M. Fernandes, S. S. Balula, L. Cunha-Silva and C. Freire, *ACS Applied Energy Materials*, 2020, **3**, 2925-2934.